SSRG International Journal of Electrical and Electronics Engineering
ISSN: 2348-8379/ https://doi.org/10.14445/23488379/IJEEE-V12I6P117

Volume 12 Issue 6, 195-205, June 2025

Original Article

Voltage Stability Assessment of a Grid-Connected Photovoltaic System Using a Combined Stability Index

Mahamat Defallah Djamaladine[1]*, Amir Moungache[2,3], Agbassou Guenoukpati[1,4], Adekunlé Akim Salami[1,4]

[1]*Centre d'Excellence Régional pour la Maîtrise de l'Electricité (CERME), University of Lome, Maritime, Togo.*
[2]*Faculté des Sciences Exactes et Appliquées, University of N'Djamena , Chari-Baguirmi, Tchad.*
[3]*Laboratoire d'Etude et de Recherche en Techniques Industrielles (LERTI), University of N'Djamena, Chari-Baguirmi, Tchad.*
[4]*Laboratoire de Recherche en Sciences de l'Ingénieur (LARSI), University of Lome, Maritime, Togo.*

Corresponding Author : jamaladinemahamat@gmail.com

Received: 12 April 2025 Revised: 14 May 2025 Accepted: 13 June 2025 Published: 30 June 2025

Abstract *- Grid-connected photovoltaic systems are subject to disturbances related to voltage changes at loads when their location is poorly chosen. Determining the injection location and evaluating the voltage stability of these networks are very important. In this work, a new method, simultaneously based on P-V and Q-V curves, called the Combined Stability Index (CSI), is proposed to evaluate the voltage stability of grid-connected photovoltaic systems. The results obtained from the CSI on the IEEE 14-bus network, with and without photovoltaic sources, confirm those of previous works. According to the different scenarios described in the article, the best location for the photovoltaic source to achieve the best voltage levels in the network is on the strongest bus. The CSI is a performance indicator that allows for the precise identification of the strengths and weaknesses of network buses better than the method based on the P-V and Q-V curves.*

Keywords *- Combined stability index, Grid-connected photovoltaic system, P-V curve, Q-V curve, Voltage stability.*

1. Introduction

Electrical energy is increasingly in demand across industries, residences, businesses, and public services. Developing countries also require higher energy consumption to sustain development [1]. Consequently, the electricity production sector must overcome significant challenges to meet this ever-growing energy demand. Indeed, global electricity generation primarily relies on fossil resources such as oil, coal, uranium, natural gas, and fuel oil. Unfortunately, electricity production from these sources emits greenhouse gases, contributing to global warming. Moreover, excessive use of these raw materials reduces available reserves, potentially resulting in their depletion by the end of this century [2], which poses obstacles to sustainable development goals. Many countries use renewable energy to address this issue, particularly by integrating photovoltaic systems into their grids. Although the increasing integration of photovoltaic generators into electrical systems helps meet rising energy demand, slows down the depletion of fossil resources, and reduces greenhouse gas emissions, it can negatively affect the grid if the photovoltaic system's integration location is poorly chosen. In such circumstances, assessing the voltage stability of the electrical network becomes necessary to identify vulnerable areas using analytical methods to ensure its proper functioning. In the literature, many methods for analyzing voltage stability have been proposed. There are traditional methods (modal analysis, continuous power flow (CPF), stability indices, as well as P-V and Q-V curves) and intelligent techniques (artificial neural networks, fuzzy logic, adaptive neuro-fuzzy inference system, and heuristic methods) [3]. Despite their numerous advantages, intelligent techniques require more data and a high computational time. That is why emphasis has been placed on traditional techniques, mainly on P-V and Q-V curves, as the former shows the system's active power transfer capacity, while the latter identifies the system's reactive power needs, ensuring stable voltage. Active power and reactive power are essential for evaluating voltage stability. Furthermore, the method based on the P-V curve and the Q-V curve has its limitations, and because of the convergence problem, for a network containing a large number of buses, its voltage stability cannot be accurately assessed.

This article aims to propose a new approach that exploits the information from the P-V and Q-V curves already plotted on the PSSE software, by looking for the tangent of each bus to make indices that will enable a global study to be made of the evaluation of voltage stability. The rest of the document is structured as follows: Section 2 presents the state of the art on existing work, followed by the methodology in Section 3. Section 4 is dedicated to the results and discussion, and Section 5 is reserved for the conclusion.

2. Literature Review on P-V and Q-V Curve Methods

For evaluating the voltage stability of grid-connected photovoltaic systems, many studies have focused on P-V and Q-V curves. In [4], the authors used modal analysis of reactive power voltage (Q-V) and real power voltage (P-V) to analyze the voltage instability of the IEEE 14-bus system. They executed the Q-V modal analysis followed by the P-V analysis. Both analyses show that bus 14 of the IEEE 14-bus system is the weakest and thus tends to produce voltage instability. However, the major drawback of this analysis is that it is complex and takes more time when applied to each bus in a large network, making it less practical for large-scale systems. The authors of the article [5] analyzed the impact of a photovoltaic connection on the IEEE 9-bus network. To choose the location of the photovoltaic source, they considered the three weakest nodes. After analysis, the authors concluded that node 5, chosen for the installation of the photovoltaic source, allows for a higher penetration level with smaller variations in the voltage profile. However, this work lacks a detailed analysis of the optimal criteria for selecting the location of the photovoltaic system.

A study was conducted to show the influence of photovoltaic systems on the voltage stability of the network in article [6]. Using the Power World simulator, the authors first analyzed the stability of the IEEE 14-bus network without a photovoltaic source, applying the P-V and Q-V curve techniques to detect the weakest buses in this network. Then, they used the concept of percentage variation in voltage-power sensitivity to determine the optimal location of the photovoltaic source in the electrical network, taking into account the effects of power factor control. However, using Power World can be time-consuming and requires significant computing resources, especially for large networks. The authors of [7] used P-V and Q-V curves to determine the active power transfer capacity and the reactive power margin to improve grid stability through series-parallel compensation. This method of assessing grid stability does not provide a comprehensive view of it.

T. Subramaniam et al. in [8] study voltage stability issues when integrating solar photovoltaic energy into the IEEE 14-bus network. The authors used a new voltage stability index to identify the weakest bus, where they injected a three-phase fault to analyze disturbances. The fault was mitigated when a photovoltaic source was connected to this bus. However, the authors did not consider the effects of load variations and weather conditions in their study. The authors' work in [9] compares voltage stability analysis using P-V and Q-V curves to time-domain simulations of converter-dominated electrical systems. According to the results obtained, Q-V analysis is generally less accurate than P-V analysis for systems incorporating power electronic converters. Taken in isolation, the P-V and Q-V curves do not precisely identify the unstable point in the network. Contrary to studies suggesting that connecting a photovoltaic system to the weakest bus can improve that bus's failure, the authors in [10] showed that the best location for photovoltaic system penetration is the strongest bus, as it does not influence other load buses. This study does not consider load variations and weather conditions.

In [11], the authors confirmed the conclusion of [10] regarding the best location for the photovoltaic system. Additionally, the Critical Voltage Sensitivity Index (CVSI) and the Critical Reactive Power Sensitivity Index (CQSI) were used to evaluate the sensitivities to voltage instability of the buses in the electrical system as the penetration level of photovoltaic systems increases. These sensitivity indices, based solely on the Q-V curve, still assess the system's voltage instability sensitivity with increasing penetration levels of photovoltaic systems, but they are insufficient due to the exclusive use of the Q-V curve. S. Rahman et al. in [12] propose a method that considers the intermittencies and uncertainties associated with PV energy sources and system loads in evaluating voltage stability using the Monte Carlo method. The results obtained from case studies (IEEE 14-bus and 30-bus networks) on the analysis of critical eigenvalues derived from the Q-V curve plotting conclude that the level of voltage stability of the network heavily depends on the location of the photovoltaic system. However, the variation in photovoltaic penetration level does not significantly impact the critical eigenvalue once the location is fixed.

According to the authors, using a single traditional technique to evaluate voltage stability is ineffective [13]. Thus, they proposed a methodology based on a combination of Q-V modal analysis, V-Q sensitivity analysis, and power voltage curves to evaluate static voltage stability analysis, taking a case study of the Kenyan electrical network. This study did not analyse the overall system stability since only the smallest eigenvalue was considered for stability evaluation.

In [14], the study presents the calculation of voltage stability margin values by measuring the hypotenuse under the P-V and Q-V curves of the IEEE 14-bus network. These voltage stability margin values are used to determine the weakest bus in the electrical system. Results obtained solely from the IEEE 14-bus network may limit the generalization of conclusions to other electrical networks.In [15], the authors examine the phenomenon of long-term voltage stability (LTVS) with large-scale solar-photovoltaic generation. Reactive power characteristics, synchronous generator (SG) and solar-PV system control schemes are carefully analysed. A rigorous analysis was carried out using a simple test system to compare the impact of solar-PV generation on the LTVS with the SG. QV curves demonstrated how the power system approaches its voltage instability point during the LTVS phenomenon. In [16], the authors examine the relationship between critical points of the P-V and V-Q curves in a simple

Thevenin equivalent system. They used theoretical and simulation analyses to identify and compare the critical points on the P-V and V-Q curves. The obtained results help identify tipping points and voltage instabilities in the Thevenin system and establish the relationship between these critical points on the two curves. The major drawback of this method is the excessive simplification of the Thevenin model, which can affect the accuracy of the results and the generalization of the conclusions.

The authors in [17] used the P-V and Q-V curves to develop voltage rise and fall indicators based on voltage sensitivity. These indicators allowed voltage stability to be quantified steadily using the IEEE 14-bus network. The simulation results indicate that buses 14, 13, and 12 are the weakest. The main limitation of this proposed method is the simplified representation of power models. E. N. Ezeruigbo et al. in [18] focus on the voltage stability analysis of the Nigerian 330 kV power grid by plotting the P-V curves of load buses to identify voltage tipping points. The study concludes that P-V curve analysis is essential for identifying critical voltage stability points and preventing power system failures. Relying solely on P-V curves, this method may not accurately reflect the network's operating conditions, affecting the precision of the results.

In [19], the authors present a method to improve the voltage stability margin by controlling power transmission paths. They used stability indices to identify weak buses and lines in the electrical system and the P-V and Q-V curves to illustrate the voltage stability margin. Two methods were employed to increase the stability margin: the first involves adding a parallel line to the system, while the second involves adding a device providing only active power, reactive power, or complex power. The results show a significant improvement in the voltage stability margin on the IEEE 30-bus test system. The methodology requires high coordination and precision in controlling power flows, which can be technically demanding and costly to implement on a large scale.

In [20], the authors present a detailed analysis of the static voltage stability of the Albanian power system using a combination of P-V and Q-V curves, a V-Q sensitivity analysis and a modal analysis. After their study, they concluded that modal analysis proved to be the most effective in locating areas vulnerable to voltage instability, providing detailed information on the weakest buses, generators and branches. The analysis is based on static methods, without taking into account the temporal dynamics of the network. In [21], the authors present a new voltage stability index based on the P-V (Power-Voltage) curve. This new index allows evaluating the grid's ability to maintain adequate voltage levels under variable load conditions. The article validates the method on distribution network models and shows that the P-V index can effectively detect critical points and help improve grid stability. This index, derived solely from P-V curves, cannot be a sufficient indicator for evaluating grid voltage stability.

As mentioned above, most studies focus on P-V or Q-V curves, or they are combined with other traditional techniques to assess the voltage stability of electrical systems. Given their limitations related to convergence issues and the use of a single bus for voltage stability analysis, P-V and Q-V curves, taken in isolation, cannot effectively evaluate the voltage stability of an electrical system. Furthermore, less effort is devoted to combining information from P-V and Q-V curves to analyze the voltage stability of electrical systems. An approach has been developed to address these shortcomings with the contributions cited below. In contrast to traditional methods that provide only a brief overview of voltage stability analysis, this work proposes a new approach based on the combined stability index, which provides a comprehensive assessment of voltage stability.

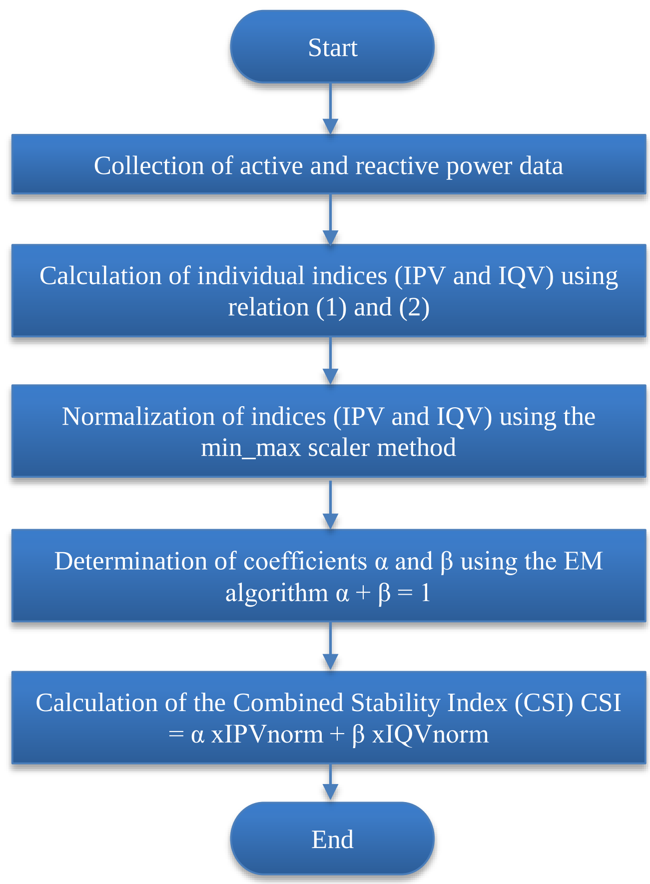

Fig. 1 Proposed algorithm for evaluating grid voltage stability

3. Materials and Methods

The methodology consists of first evaluating the voltage stability of the IEEE 14-bus network, followed by the analysis of the voltage stability of a photovoltaic source connected to this network. Figure 1 presents the methodology used in this study. It involves several steps described as follows: The IEEE 14-bus network is chosen and modelled for data collection in the PSSE software environment. Next, a power flow calculation is performed using the Newton-Raphson method to get a general idea of the network's behavior through the slack bus or reference node. Finally, the simulation data is exported to Python to represent the P-V and Q-V curves of the various load buses in the network. Additionally, this data is used to calculate the individual active and reactive indices according to equations 1 and 2.

$$IPV_i = \frac{\Delta V}{\Delta P} = \frac{V_i - V_{i-1}}{P_i - P_{i-1}} \quad (1)$$

$$IQV_i = \frac{\Delta V}{\Delta Q} = \frac{V_i - V_{i-1}}{Q_i - Q_{i-1}} \quad (2)$$

Where: ΔV is the voltage variation, ΔP is the active power variation, ΔQ is the reactive power variation, IPVi is the active index of bus i, and IQVi is the reactive index of bus I After calculating the individual active and reactive indices, their normalization procedure is performed according to equations 3 and 4.

$$IPV_{norm} = \frac{IPV - IPV_{min}}{IPV_{max} - IPV_{min}} \quad (3)$$

$$IQV_{norm} = \frac{IQV - IQV_{min}}{IQV_{max} - IQV_{min}} \quad (4)$$

Where: IPVnorm is the normalized active index, IPVmin is the minimum active index, IPVmax is the maximum active index, IQVnorm is the normalized reactive index, IQVmin is the minimum reactive index, and IQVmax is the maximum reactive index Finally, the normalized indices are combined to obtain the Combined Stability Index (CSI) for each bus according to equation (5). The CSI is a weighted average of the normalized IPV and IQV indices.

$$CSI = \alpha \times IPV_{norm} + \beta \times IQV_{norm} \quad (5)$$

With α and β, the weighting coefficients such that α + β =1

3.1. Study Data Description

The data used in this study comes from the IEEE 14-bus network [7]. This network, presented in Figure 2, includes two generation nodes, one of which is a slack bus, three synchronous condensers modeled in PSSE as continuous shunt elements, fourteen buses, seventeen branches, and three two-winding transformers. The slack bus's load is 259 MW and 73.5 MVAR. The network has three voltage levels: buses 1, 2, 3, 4, and 5 have a voltage of 132 kV. The other buses have a voltage of 33 kV, except for bus 8, which has a voltage of 11 kV. For the active and reactive power of the photovoltaic source, the study was based on the reference bus, which regulates the network's operation in terms of both active and reactive power. To this end, a range of 5% to 50% of the active and reactive power of the reference bus was considered to determine the size of the photovoltaic source. The line parameters are based on those of the bus to which this photovoltaic source is connected. The parameters of the buses, generators, loads, lines, and transformers are presented in Tables 1, 2, and 3.

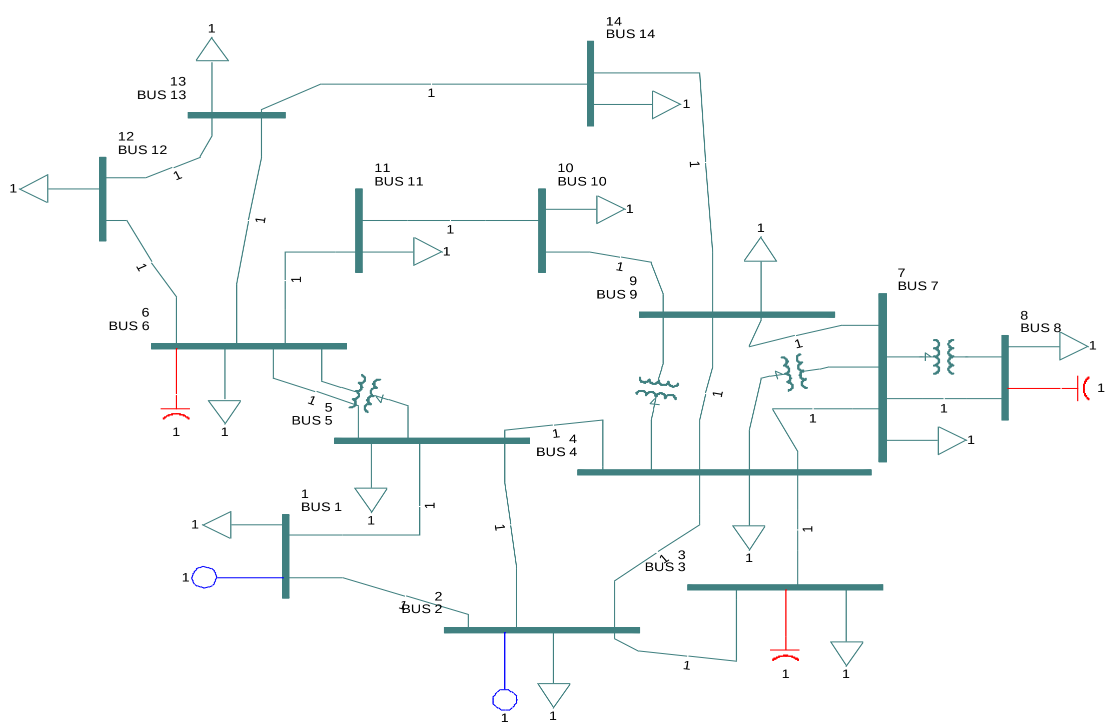

Fig. 2 IEEE 14-bus network

Table 1. Network parameters: bus, generator and load parameters [7]

Bus data				Generators and synchronous condensers				Loads	
Bus No.	**Bus code**	**Bus voltage (PU)**	**Bus angle (deg)**	**P_G (MW)**	**Q_G (MVAr)**	**Q_{min} (MVAr)**	**Q_{max} (MVAr)**	**P_L (MW)**	**Q_L (MVAr)**
1	**1**	1.06	0	0	0	0	0	0	0
2	**2**	1.045	0	40	42.4	-40	50	21.7	12.7
3	**2**	1.01	0	0	23.4	0	40	94.2	19
4	**3**	1.0	0	0	0	0	0	47.8	-3.9
5	**3**	1.0	0	0	0	0	0	7.6	1.6
6	**2**	1.07	0	0	12.2	-6	24	11.2	7.5
7	**3**	1.0	0	0	0	0	0	0	0
8	**2**	1.0	0	0	17.4	-6	24	0	0
9	**3**	1.0	0	0	0	0	0	29.5	16.6
10	**3**	1.0	0	0	0	0	0	9.0	5.8
11	**3**	1.0	0	0	0	0	0	3.5	1.8
12	**3**	1.0	0	0	0	0	0	6.1	1.6
13	**3**	1.0	0	0	0	0	0	13.5	5.8
14	**3**	1.0	0	0	0	0	0	14.9	5

Table 2. Network components rating [7]

Power Factor	Maximum Generated Power (MW)
Gen 1	615
Gen 2	100
Transformer 5-6	100
Transformer 4-9	100
Transformer 4-7	100

Table 3. Network parameters: transmission lines and transformers [7]

From bus	To bus	R (p.u)	X (p.u)	B/2 (p.u)	Transformer Tap
1	**2**	0.01938	0.05917	0.0264	1
1	**5**	0.05403	0.22304	0.0246	1
2	**3**	0.04699	0.19797	0.0219	1
2	**4**	0.05811	0.17632	0.0170	1
2	**5**	0.05695	0.17388	0.0173	1
3	**4**	0.06701	0.17103	0.0064	1
4	**5**	0.01335	0.04211	0.0000	1
4	**7**	0.00000	0.20912	0.0000	0.978
4	**9**	0.00000	0.55618	0.0000	0.969
5	**6**	0.00000	0.25202	0.0000	0.932
6	**11**	0.09498	0.19890	0.0000	1
6	**12**	0.12291	0.25581	0.0000	1
6	**13**	0.06615	0.13027	0.0000	1
7	**8**	0.03181	0.17615	0.0000	1
7	**9**	0.00000	0.11001	0.0000	1
9	**10**	0.03181	0.08450	0.0000	1
9	**14**	0.12711	0.27038	0.0000	1
10	**11**	0.08205	0.19207	0.0000	1
12	**13**	0.22092	0.19988	0.0000	1
13	**14**	0.17093	0.34802	0.0000	1

4. Results and Discussion

Based on the simulation results in Figure 3, a comparison is made between the actual and measured or simulated values of the load voltages. Bus 14 has the lowest voltage with an estimated voltage drop of 3.56%, followed by buses 13 and 12 with voltage drops of 2.58% and 2.14%, respectively. For the evaluation of voltage stability, the buses considered are those with loads. Figures 4 and 5 present the simulation results of the P-V and Q-V curves.

According to Figure 4, the P-V curves show that as active power increases, voltage decreases. Beyond the value of 200 MW, the limit point begins, beyond which the system enters the instability zone corresponding to a voltage of 0.9 p.u. for all buses, except for buses 14, 13, and 12, which have a voltage below 0.9 p.u. It is also noted that bus 14 is the weakest bus, followed by buses 13 and 12. These buses are the first to reach the instability zone, especially bus 14, making it the element that can cause the most instability in the network. It is also worth noting that bus 5 has the highest voltage in the network.

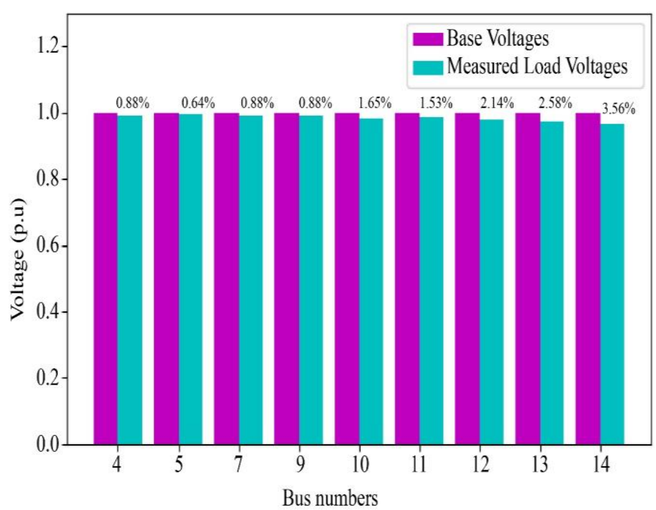

Fig. 3 Comparison of input voltages and measured load voltages

Regarding the Q-V curves (Figure 5), reactive power increases with voltage up to the normal operating point (1.1 p.u), indicating that the system is stable. However, it is observed that bus 14 has a low reactive power margin compared to other buses, followed by bus 12 and then bus 13.

Additionally, bus 5 has the largest reactive power margin. Typically, voltage stability evaluation from these curves is done separately. In the following part of this work, a new method is proposed for a more global analysis of voltage stability based on the combined stability index. Tables 4 and 5 present the normalization results of the IPV and IQV indices.

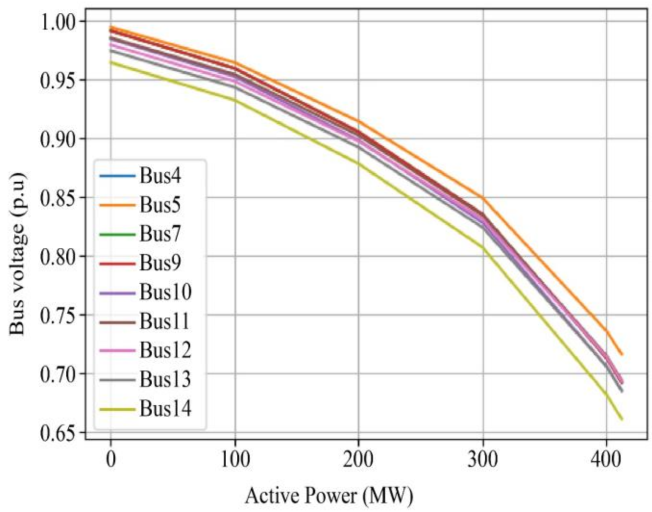

Fig. 4 Result of PV curve

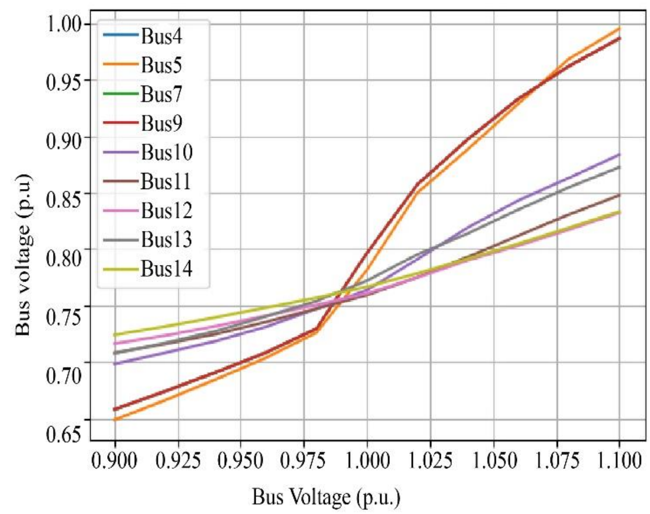

Fig. 5 Result of QV curve

Table 4. Normalized IPV indices

Bus	$IPV1_{norm}$	$IPV2_{norm}$	$IPV3_{norm}$
Bus 4	0.00032	0.00070	0.00168
Bus 5	0.00030	0.00065	0.00160
Bus 7	0.00032	0.00070	0.00168
Bus 9	0.00032	0.00070	0.00168
Bus 10	0.00032	0.00070	0.00168
Bus 11	0.00031	0.00068	0.00168
Bus 12	0.00031	0.00066	0.00168
Bus 13	0.00031	0.00068	0.00168
Bus 14	0.00032	0.00071	0.00168

Table 4. Normalized IQV indices

Bus	$IQV1_{norm}$	$IQV2_{norm}$	$IQV3_{norm}$	$IQV4_{norm}$	$IQV5_{norm}$	$IQV6_{norm}$
Bus 4	0.000814	0.000560	0.000329	0.000945	0.001192	0.001258
Bus 5	0.000747	0.000497	0.000293	0.000900	0.001092	0.001151
Bus 7	0.000815	0.000560	0.000329	0.000950	0.001193	0.001259
Bus 9	0.000814	0.000560	0.000330	0.000943	0.001193	0.001259
Bus 10	0.000971	0.000833	0.000733	0.001260	0.001944	0.002045
Bus 11	0.001173	0.001063	0.001268	0.001723	0.002312	0.002541
Bus 12	0.001340	0.001533	0.001416	0.002073	0.002378	0.002829
Bus 13	0.001120	0.000947	0.000864	0.001470	0.001901	0.002201
Bus 14	0.001384	0.001489	0.001696	0.002252	0.002481	0.002699

To calculate the combined stability indices, it is important to determine the weighting coefficients α and β, associated respectively with the weights of the IPV and IQV indices.

To achieve this,

The Expectation-Maximisation algorithm is used [22]. The results obtained give:

$\alpha = 0.0043185$ and $\beta = 0.9956814$. These values are used to calculate the CSI presented in Table 6.

Table 5. Combined stability indices

Bus	CSI	Rank
Bus 4	5.1×10^{-3}	2
Bus 5	4.7×10^{-3}	1
Bus 7	5.1×10^{-3}	3
Bus 9	5.1×10^{-3}	4
Bus 10	7.8×10^{-3}	5
Bus 11	1.01×10^{-2}	7
Bus 12	1.16×10^{-2}	8
Bus 13	8.5×10^{-3}	6
Bus 14	1.20×10^{-2}	9

Based on the analysis of the results in Table 6, the combined stability indices provide a global overview of the strengths and weaknesses of the buses. A high CSI indicates low voltage stability, while a low CSI indicates better voltage stability. From Table 6, it is evident that bus 14 is the weakest, followed by buses 12 and 11, with bus 5 being the strongest, contrary to the study by [2], which, based solely on the P-V curve, ranks the bus weaknesses as follows: 14, 13, 12, with bus 5 being the strongest. The same conclusion was reached using the P-V curves. However, with the CSI, which is based on information from both P-V and Q-V curves, these results are more reliable.

Two choices were made to determine the location of the photovoltaic source. The first involves injecting the photovoltaic source into the three weakest buses (buses 14, 13, and 12). The second involves connecting this photovoltaic source to the strongest bus (bus 5). The choice of active and reactive power of the photovoltaic source is made according to the slack bus or reference bus of the IEEE 14-bus network without the photovoltaic source. The optimal power factor adopted is 0.98, which provides fewer voltage drops at the load buses. The active and reactive power generated by the slack bus of the IEEE 14-bus network without photovoltaic sources are as follows:

PG = 234.6 MW and QG = -51.4 MVAR.

It should be noted that several configurations are considered when choosing the photovoltaic source location. In the first configuration, the photovoltaic source is injected at bus 14. The penetration rates corresponding to values of 5%, 10%, 15%, 20%, 30%, 40%, and 50% of the generated active power and generated reactive power of the slack bus constitute the active and reactive power of the photovoltaic source. The variations in the voltages of the load buses according to the level of photovoltaic penetration are presented in Figure 6.

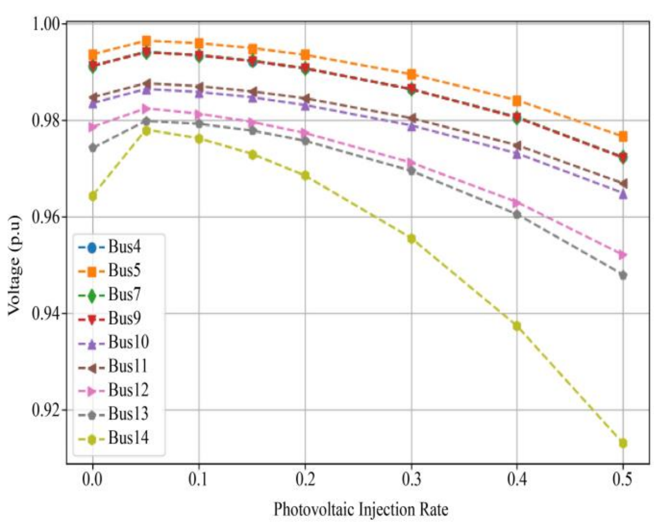

Fig. 6 Measured load bus voltages with photovoltaic injection

The second configuration involves connecting the photovoltaic source to bus 13. The same principle for choosing the active and reactive power of the photovoltaic source described in the first configuration is applied here. The results are presented in Figure 7. In the third configuration, the penetration of the photovoltaic source is made at bus 12. The principle described in configuration 1 is applied here as well. The results are presented in Figure 8.

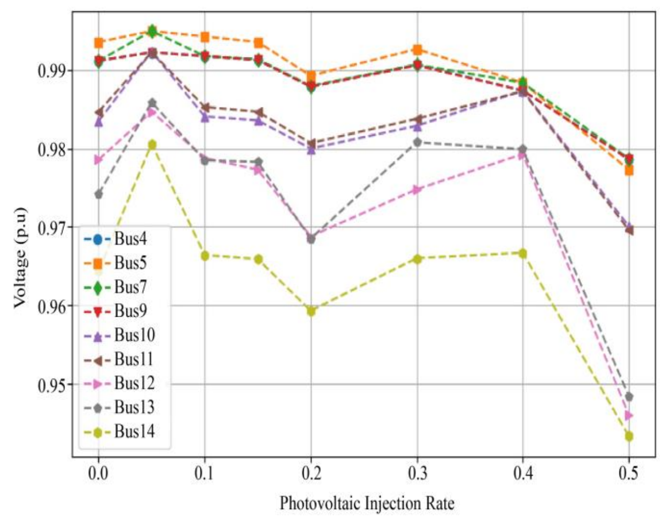

Fig. 7 Measured load bus voltages with photovoltaic injection

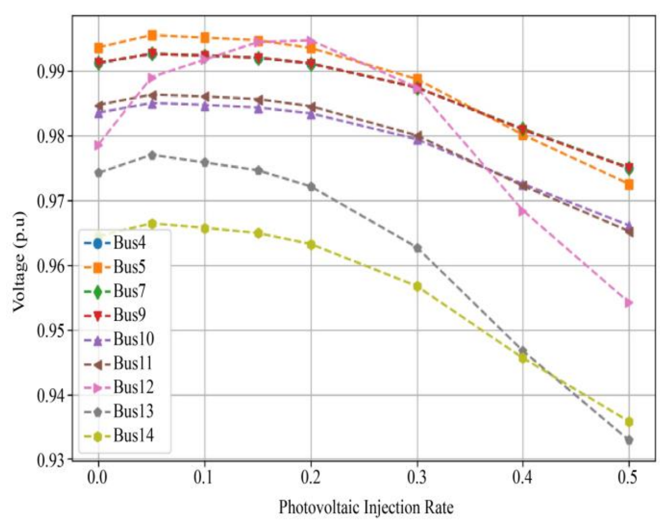

Fig. 8 Measured load bus voltages with photovoltaic injection

Based on Figure 6, 7, and 8, it is observed that the favorable photovoltaic penetration rate for improving the various load bus voltages in the IEEE 14-bus network is 5%. With this rate, the different voltages for Figures 6 and 7 in configurations 1 and 2 have an amplitude around 0.98 p.u. Even the weakest bus, bus 14, saw its voltage increase to approximately 0.98 p.u., contrary to the IEEE 14-bus network without photovoltaic injection, where a voltage of 0.96 p.u. is recorded at the same bus. Buses 14, 13, and 12 are the weakest in all three configurations, and bus 5 is the strongest.

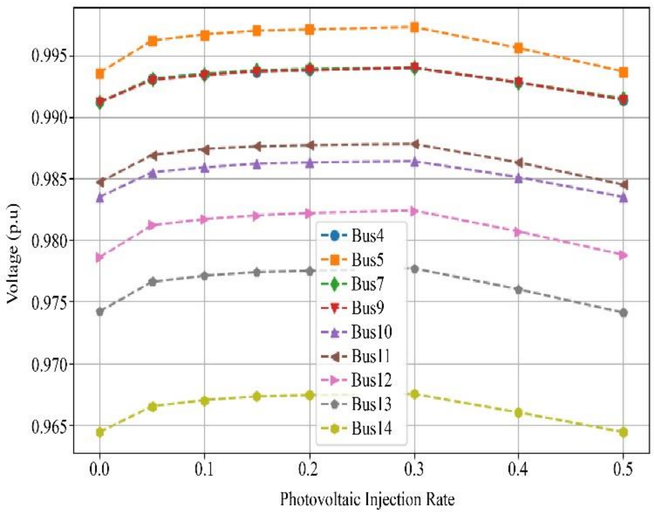

Fig. 9 Measured load bus voltages with photovoltaic injection

However, in the third scenario, the contribution of photovoltaic injection is almost insignificant for bus 14.

In the fourth configuration, the photovoltaic source is connected to the strongest bus, bus 5, following the same photovoltaic penetration principle described in the first configuration. The results are presented in Figure 9.

Figure 9 shows a progression of bus voltage amplitudes as the photovoltaic penetration rate increases. At 30%, the voltage amplitudes start to drop.

Thus, the optimal rate retained is 30%. The results obtained from the different configurations show that the best location to connect a photovoltaic source to the network is at bus 5. This conclusion confirms those in [10, 11].

4.1. Evaluation of the Stability of the IEEE 14-Bus System with Photovoltaic Injection

In this context, load buses are also considered for evaluation of the voltage stability of the IEEE 14-bus network. Figure 10 presents the IEEE 14-bus network with photovoltaic injection at bus 5.

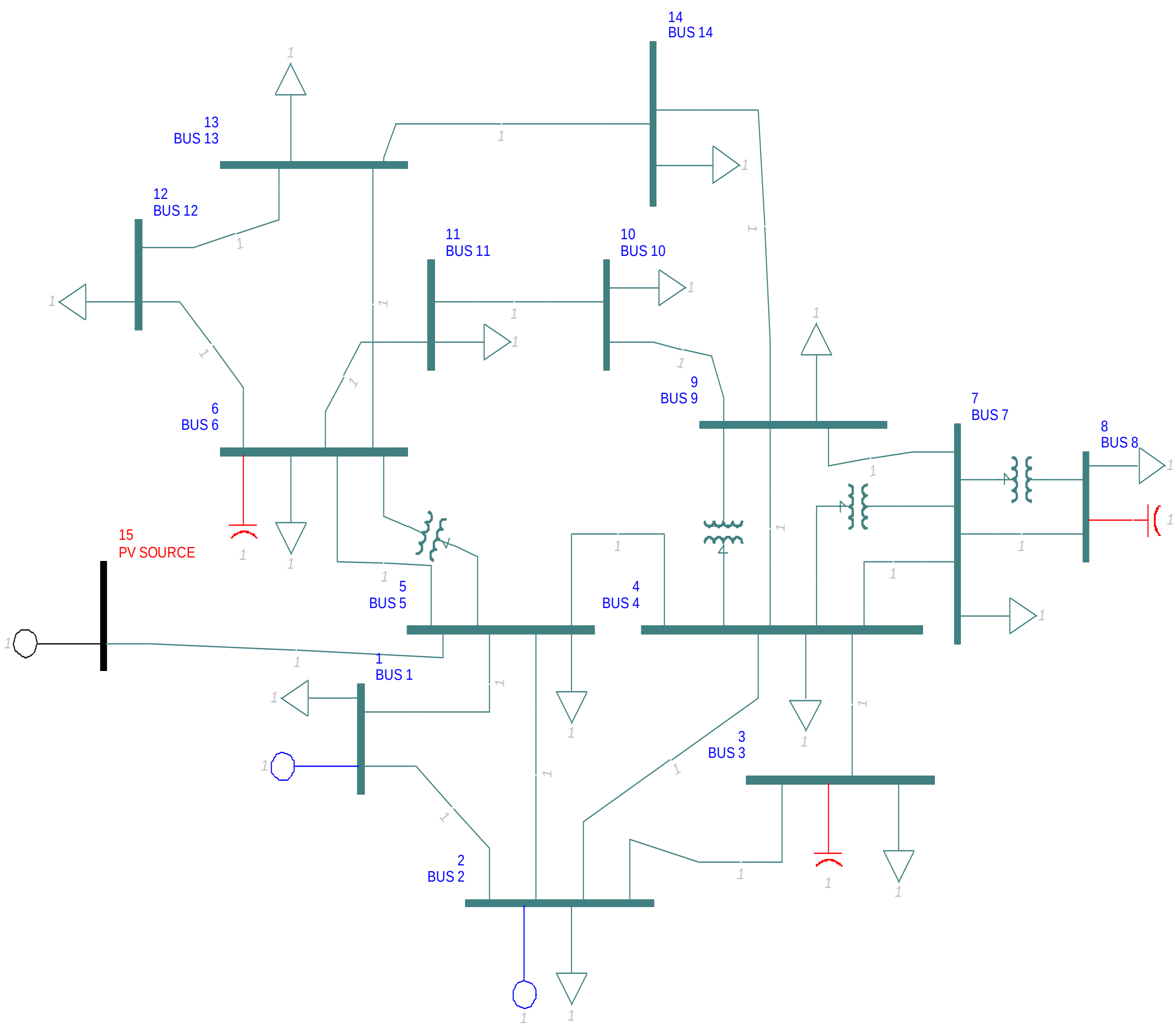

Fig. 10 IEEE 14-bus network with photovoltaic source

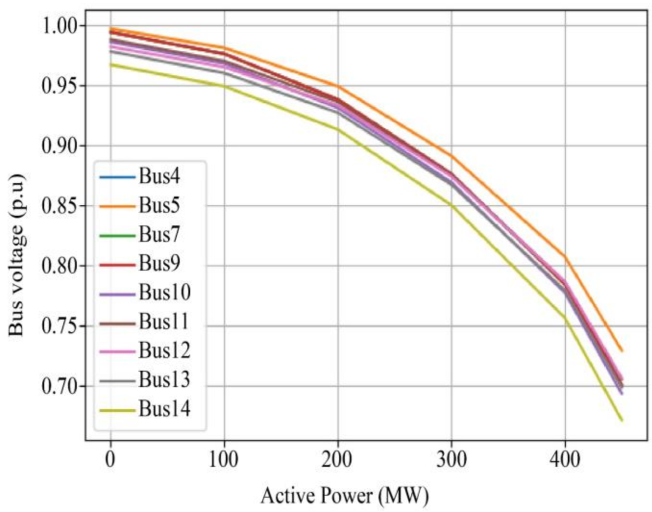

Fig. 11 Result of PV curve

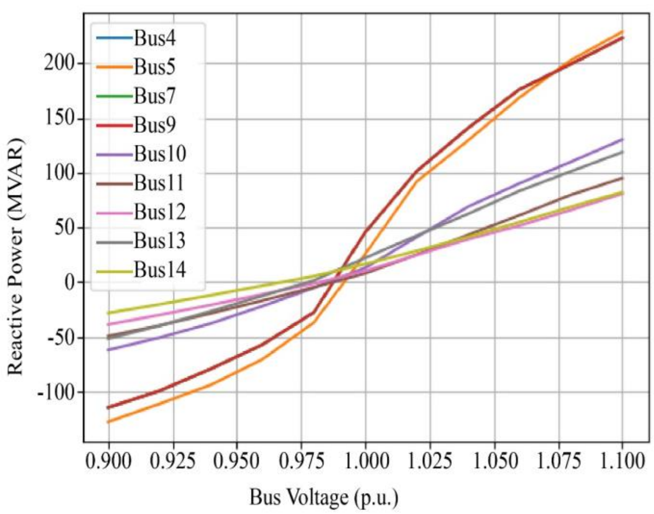

Fig. 12 Result of QV curve

The simulation results for evaluating voltage stability using the P-V and Q-V curve methods are presented in Figures 11 and 12 Referring to the P-V curve in Figure 11, we observe that as active power increases, voltage drops. Unlike the evaluation of the stability of the IEEE 14-bus network without photovoltaic injection, where the maximum transfer power was 200 MW and the lowest voltage was below 0.9 p.u., here, the transfer power beyond which the system enters the instability zone is equal to 230 MW, and the lowest voltage at this level is 0.90 p.u. Therefore, the maximum power that can be transferred is 230 MW instead of 200 MW, as was the case with the IEEE 14-bus network without photovoltaic injection.

Regarding the QV curve (Figure 12), load voltages increase with reactive powers, indicating system stability. It should also be noted that bus 12 has the lowest reactive power margin, followed by buses 14 and 11. The photovoltaic insertion has slightly changed the order of the weak buses, but bus 5, with a large reactive power margin, remains the strongest bus. Following this voltage stability evaluation using P-V and Q-V curves, the next step will be to apply the new method for a more global evaluation of the photovoltaic system connected to the network. Tables 7 and 8 present the normalization results of the IPV and IQV indices.

Table 6. Normalized IPV indices

Bus	$IPV1_{norm}$	$IPV2_{norm}$	$IPV3_{norm}$
Bus 4	0.00018	0.00062	0.00084
Bus 5	0.00016	0.00058	0.00078
Bus 7	0.00018	0.00062	0.00084
Bus 9	0.00018	0.00062	0.00084
Bus 10	0.00018	0.00062	0.00084
Bus 11	0.00018	0.00061	0.00081
Bus 12	0.00017	0.00059	0.00080
Bus 13	0.00018	0.00060	0.00081
Bus 14	0.00018	0.00063	0.00085

Table 7. Normalized IQV indices

Bus	$IQV1_{norm}$	$IQV2_{norm}$	$IQV3_{norm}$	$IQV4_{norm}$	$IQV5_{norm}$	$IQV6_{norm}$
Bus 4	0.000833	0.000566	0.000358	0.000679	0.000992	0.001308
Bus 5	0.000774	0.000510	0.000303	0.000593	0.001150	0.001218
Bus 7	0.000836	0.000566	0.000358	0.000682	0.000994	0.001307
Bus 9	0.000836	0.000567	0.000359	0.000678	0.000993	0.001308
Bus 10	0.000980	0.000939	0.000713	0.001200	0.001535	0.001779
Bus 11	0.001308	0.001115	0.001169	0.001643	0.001803	0.002062
Bus 12	0.001348	0.001608	0.001381	0.002014	0.002181	0.002299
Bus 13	0.001140	0.000951	0.000983	0.001415	0.001503	0.001691
Bus 14	0.001493	0.001488	0.001685	0.002281	0.002401	0.002528

To calculate the combined stability indices, determining the values of the weighting coefficients α and β, associated respectively with the weights of the IPV and IQV indices, is necessary. To achieve this, the EM algorithm is used [22]. The results obtained give $\alpha = 0.0008737$ and $\beta = 0.9991262$. These values are used to calculate the ISC presented in Table 9.

Table 8. Combined stability indices

Bus	CSI	Rank
Bus 4	7.8912×10^{-4}	2
Bus 5	7.5778×10^{-4}	1
Bus 7	7.9029×10^{-4}	3
Bus 9	7.8995×10^{-4}	4

Bus 10	1.2×10^{-3}	5
Bus 11	1.5×10^{-3}	7
Bus 12	1.8×10^{-3}	8
Bus 13	1.3×10^{-3}	6
Bus 14	2.0×10^{-3}	9

According to Table 9, the combined stability indices provide a global overview of the strengths and weaknesses of the buses. A high CSI indicates low voltage stability, while a low CSI indicates better stability. From this table, bus 14 is the weakest, followed respectively by buses 12 and 11, with bus 5 being the strongest. However, the insertion of the photovoltaic source into the network has particularly benefited bus 13, which now ranks as the sixth strongest bus.

5. Conclusion

Like other traditional methods, the P-V and Q-V curves are used to assess the voltage stability of electrical systems. However, their analysis is not comprehensive. For this reason, a new method based on these graphs, which produces an index called the Combined Stability Index (CSI), has been proposed in this work, offering a more comprehensive view of voltage stability. Furthermore, the weighting coefficients α and β can be adjusted to reflect the relative importance of the P-V and Q-V indices in different situations. The CSI thus allows for the precise identification of buses that require improvements to maintain the voltage stability of the network. The simulation results obtained using the combined stability index (CSI) method for the strength and weakness of the IEEE 14-bus network confirm the robustness of the method, as it has yielded almost the same results as those obtained by several other authors. Once the best location for the photovoltaic source has been determined, the CSI-based method was applied to re-evaluate the stability of the IEEE 14-bus network connected to the photovoltaic source.

The insertion of the photovoltaic system into the network has raised the voltage levels of all load buses and delayed the stability limit point. In this case, the CSI enabled us to identify the strengths and weaknesses of the IEEE 14 bus network. However, this study did not consider the intermittency of photovoltaic production and harmonic disturbances.

In sum, the ISC is a performance indicator that enables network managers to effectively evaluate the voltage stability of photovoltaic systems connected to the network.

Acknowledgments

The authors would like to thank the CERME of the University of Lomé for its multifaceted support, which made this work possible.

References

[1] Tong Zhu et al., "Analysis and Suppression of Harmonic Resonance in Photovoltaic Grid-Connected Systems," *Energies*, vol. 17, no. 5, pp. 1-22, 2024. [CrossRef] [Google Scholar] [Publisher Link]

[2] Sandra Bouneau et al., "Simplified Construction of an Energy World in 2050," *Physical Reflections*, no. 1, pp. 30-35, 2013. [CrossRef] [Google Scholar] [Publisher Link]

[3] Xinyu Liang, Hua Chai, and Jayashri Ravishankar, "Analytical Methods of Voltage Stability in Renewable Dominated Power Systems: A Review," *Electricity*, vol. 3, no. 1, pp. 75-107, 2022. [CrossRef] [Google Scholar] [Publisher Link]

[4] Ahmad Fateh Mohamad Nor, and Marizan Sulaiman, "Voltage Stability Assessment of Power System Network using QV and PV Modal Analysis," *Journal of Telecommunication, Electronic and Computer Engineering (JTEC)*, vol. 8, no. 7, pp. 7-11, 2016. [Google Scholar] [Publisher Link]

[5] G. Maliki et al., "Analysis of the Impacts of Increased Penetration of Electricity Networks by Photovoltaic Generators," *Maghrebian Journal of Pure and Applied Science*, vol. 8, no. 2, pp. 111-121, 2022. [CrossRef] [Google Scholar] [Publisher Link]

[6] Abdullahi Oboh Muhammed, and Muhyaddin Rawa, "A Systematic PVQV-Curves Approach for Investigating the Impact of Solar Photovoltaic-Generator in Power System Using PowerWorld Simulator," *Energies*, vol. 13, no. 10, pp. 1-21, 2020. [CrossRef] [Google Scholar] [Publisher Link]

[7] Rahul Kumar et al., "PV and QV Curve Analysis Using Series and Shunt Compensation," *2020 IEEE 9th Power India International Conference (PIICON)*, Sonepat, India, pp. 1-6, 2020. [CrossRef] [Google Scholar] [Publisher Link]

[8] Tenarasi Subramaniam et al., "An Investigation on the Power System Stability of Photovoltaic Grid Integrated System," *2017 7th IEEE International Conference on Control System, Computing and Engineering (ICCSCE)*, Penang, Malaysia, pp. 356-359, 2017. [CrossRef] [Google Scholar] [Publisher Link]

[9] V.N. Sewdien et al., "Evaluation of PV and QV Based Voltage Stability Analyses in Converter Dominated Power Systems," *2018 IEEE PES Asia-Pacific Power and Energy Engineering Conference (APPEEC)*, Kota Kinabalu, Malaysia, pp. 161-165, 2018. [CrossRef] [Google Scholar] [Publisher Link]

[10] M.H. Ibrahim et al., "Voltage Stability Assessment for Solar Photovoltaic Penetration Using Reactive Power-Voltage and Active Power-Voltage Modal Analysis," *Energy Reports*, vol. 9, pp. 486-493, 2023. [CrossRef] [Google Scholar] [Publisher Link]

[11] Bukola Babatunde Adetokun, Joseph Olorunfemi Ojo, and Christopher Maina Muriithi, “Reactive Power-Voltage-Based Voltage Instability Sensitivity Indices for Power Grid with Increasing Renewable Energy Penetration,” *IEEE Access*, vol. 8, pp. 85401-85410, 2020. [CrossRef] [Google Scholar] [Publisher Link]

[12] S. Rahman et al., “Analysis of Power Grid Voltage Stability with High Penetration of Solar PV Systems,” *IEEE Transactions on Industry Applications*, vol. 57, no. 3, pp. 2245-2257, 2021. [CrossRef] [Google Scholar] [Publisher Link]

[13] Ombuki Mogaka, Roy Orenge, and Julius Ndirangu, “Static Voltage Stability Assessment of the Kenyan Power Network,” *Journal of Electrical and Computer Engineering*, vol. 2021, pp. 1-16, 2021.[CrossRef] [Google Scholar] [Publisher Link]

[14] Ahmad Fateh Mohamad Nor et al., “Determining Voltage Stability Margin Values by Measuring the Hypotenuse Under PV and QV Curves,” *International Journal of Electrical Engineering and Applied Sciences (IJEEAS)*, vol. 1, no. 1, pp. 25-30, 2018. [Google Scholar] [Publisher Link]

[15] E. Munkhchuluun, L. Meegahapola, and A. Vahidnia, “Long-Term Voltage Stability with Large-Scale Solar-Photovoltaic (PV) Generation,” *International Journal of Electrical Power & Energy Systems*, vol. 117, 2020. [CrossRef] [Google Scholar] [Publisher Link]

[16] Xuan Li et al., “Study on the Corresponding Relationship between Critical Points of P-V Curve and V-Q Curve of Simple Thevenin Equivalent System,” *2020 IEEE 1st China International Youth Conference on Electrical Engineering (CIYCEE)*, Wuhan, China, pp. 1-7, 2020. [CrossRef] [Google Scholar] [Publisher Link]

[17] Xuan Zhang et al., “Steady-State Voltage Stability Assessment of New Energy Power Systems with Multi-Quadrant Power Modes,” *Energy Reports*, vol. 9, pp. 3851-3860, 2023. [CrossRef] [Google Scholar] [Publisher Link]

[18] E.N. Ezeruigbo, A.O. Ekwue, and L.U. Anih, “Voltage Stability Analysis of Nigerian 330kV Power Grid using Static P-V Plots,” *Nigerian Journal of Technology*, vol. 40, no. 1, pp. 70-80, 2021. [CrossRef] [Google Scholar] [Publisher Link]

[19] Ahmed Nasser B. Alsammak, and Maan Hussein A. Safar, “Voltage Stability Margin Improving by Controlling Power Transmission Paths,” *International Journal of Engineering and Innovative Technology (IJEIT)*, vol. 7, no. 1, pp. 26-32, 2017. [Google Scholar] [Publisher Link]

[20] Viktor Rrotani, Rajmonda Bualoti, and Marialis Çelo, “Static Voltage Stability Analysis with the Integration of Distributed Generation: An Albanian Case Study,” *WSEAS Transactions on Power Systems*, vol. 19, pp. 427-437, 2024. [CrossRef] [Google Scholar] [Publisher Link]

[21] Sheng Li, Yuan Gao, and Chengcheng Jiang, “A Static Voltage Stability Index Based on P-V Curve for the Medium-Voltage Distribution Network with Distributed PV,” *Journal of Physics: Conference Series, The 6th International Conference on Mechanical, Electric, and Industrial Engineering (MEIE 2023)*, Sanya, China, vol. 2591, no. 1, pp. 1-7, 2023. [CrossRef] [Google Scholar] [Publisher Link]

[22] Zhihua Zhang et al., “EM Algorithms for Gaussian Mixtures with Split-and-Merge Operation,” *Pattern Recognition*, vol. 36, no. 9, pp. 1973-1983, 2003. [CrossRef] [Google Scholar] [Publisher Link]